(46) P. J. Flory, ref 42, p 35.
(47) G. Allen, D. C. W. Morley, and T. Williams, *J. Mater. Sci.*, **8**, 1449 (1973).
(48) G. A. Adam, A. Cross, and R. N. Haward, *J. Mater. Sci.*, **10**, 1582 (1975).
(49) R. J. Morgan and J. E. O'Neal, *J. Polym. Sci., Polym. Phys.*, **14**, 1053 (1976).
(50) A. E. Tonelli, *Macromolecules*, **4**, 653 (1971).
(51) P. Botherel and G. Fourche, *J. Chem. Soc., Faraday Trans. 2*, **69**, 441 (1973).
(52) P. J. Flory, *Macromol. Chem.*, **8**, 1 (1973); reprinted as *Rub. Chem. Technol.*, **48**, 513 (1975).
(53) R. F. Boyer, *J. Macromol. Sci., Phys.*, in press.
(54) E. W. Fischer, J. H. Wendorff, M. Dettenmaier, G. Lieser, and I. Voigt-Martin, *Polym. Prepr., Am. Chem. Soc., Div. Polym. Chem.*, **15**(2), 8 (1974).
(55) H. Benoit, *Polym. Prepr., Am. Chem. Soc., Div. Polym. Chem.*, **15**(2), 324 (1974).
(56) A. Pines, M. G. Gibby, and J. S. Waugh, *Chem. Phys. Lett.*, **15**, 373 (1972).
(57) J. Heijboer, "Physics of Non-crystalline Solids", North-Holland Publishing Co., Amsterdam, 1965.
(58) A. E. Tonelli, *Macromolecules*, **5**, 558 (1972). However, quite different results have been obtained by other calculations. See, for example, F. Laupretre and L. Monnerie, *Eur. Polym. J.*, **10**, 21 (1974).
(59) See, for example, ref 9, p 182.
(60) For recent reviews, see R. F. Boyer, *Polym. Eng. Sci.*, **8**(3), 161 (1968); J. A. Sauer, *J. Polym. Sci., Part C*, **32**, 69 (1971); R. F. Boyer, "Polymeric Materials", American Society of Metals, Metals Park, Ohio, 1975, p 277; P. I. Vincent, *Polymer*, **15**, 111 (1974).
(61) H. Heijboer, *Kolloid-Z.*, **171**, 7 (1960); L. E. Nielsen, "Mechanical Properties of Polymers", Van Nostrand-Reinhold, Princeton, N.J., 1962, p 209.
(62) Reference 9, p 127.
(63) Reference 9, p 125.
(64) Y. Ishida, *Kolloid-Z.*, **174**, 124 (1961).
(65) W. E. Wolstenholme, *J. Appl. Polym. Sci.*, **6**, 332 (1962).
(66) J. C. Radon and C. E. Turner, *Eng. Fract. Mech.*, **1**, 411 (1969).
(67) F. A. Johnson, A. P. Glover, and J. C. Radon, "Symposium on the Mechanical Behavior of Materials", Material Science, Japan, 1974, p 141.
(68) L. C. Cessna, *Polym. Prepr., Am. Chem. Soc., Div. Polym. Chem.*, **15**, 229 (1974).
(69) See, for example, E. H. Andrews, "Fracture in Polymers", Elsevier, New York, N.Y., 1968, p 71.
(70) A. Papoulis, "Probability, Random Variables, and Stochastic Processes", McGraw-Hill, New York, N.Y., 1965, p 338.
(71) A. Abragam, "Principles of Nuclear Magnetism", Oxford, 1961, p 271.
(72) Typical reservations are expressed by G. E. Roberts and E. F. T. White, "The Physics of Glassy Polymers", R. N. Haward, Ed., Applied Science, London, 1973, p 194; and I. M. Ward, "Mechanical Properties of Solid Polymers", Wiley, New York, N.Y., 1971, p 334.
(73) S. S. Sternstein, ref 16, p 369.
(74) A. S. Argon, ref 16, p 411.
(75) J. Schaefer, *Bull. Am. Phys. Soc.*, **21**, 443 (1976).
(76) D. Hull, ref 16, p 487.
(77) J. S. Waugh as cited in L. Müler, A. Kumar, and R. R. Ernst, *J. Chem. Phys.*, **63**, 5490 (1975); R. K. Hester, J. L. Ackerman, B. L. Neff, and J. S. Waugh, *Phys. Rev. Lett.*, **36**, 1081 (1976).

Molecular and Crystal Structures of Poly(ethylene oxybenzoate): α Form

Hiroshi Kusanagi, Hiroyuki Tadokoro,* Yozo Chatani, and Kazuaki Suehiro[1]

Department of Polymer Science, Faculty of Science, Osaka University, Toyonaka, Osaka 560, Japan. *Received August 11, 1976*

ABSTRACT: The crystal structure of poly(ethylene oxybenzoate) α form was determined by x-ray analysis and intra- and intermolecular interaction potential energy calculations, i.e., the crystal structure model was refined by using a packing energy minimization method prior to the least-squares refinement in x-ray analysis. The unit cell is orthorhombic, $P2_12_12_1$, with a = 10.49 Å, b = 4.75 Å, and c (fiber axis) = 15.60 Å. The two antiparallel (2/1) helical chains are located at the center and the corner of the unit cell. The internal rotation angles are

$$\text{——CH}_2\text{——(——O——Ph——CO——O——CH}_2\text{——CH}_2\text{——)——}$$
$$-186^\circ \qquad -13^\circ \ -15^\circ \ -172^\circ \ -102^\circ \ -59^\circ$$

where the angle (−13°) is for the virtual bond (O–Ph–C) and the dihedral angle (−15°) is defined by the planes of the benzene ring and the ester group. The chain has a zigzag conformation of large scale, one monomeric unit being a large zigzag unit. The low crystallite modulus of the α form is explained by this molecular structure.

Poly(ethylene oxybenzoate), $[-OPhCOOCH_2CH_2-]_n$, is an aromatic poly(ester ether), the chemical structure of which is similar to poly(ethylene terephthalate), $[-OCOPhCOOCH_2CH_2]_n$. The only difference is at the linkage adjacent to the aromatic ring (left side in the formula): ether or ester. This difference, however, leads to the remarkable difference of the molecular conformations and crystal structures, which should be reflected in the various physical properties. Poly(ethylene terephthalate) has an almost fully extended molecular conformation in the crystal[2] and the high crystallite modulus 108 × 10^{10} dyn/cm^2.[3] On the other hand, poly(ethylene oxybenzoate) has two crystal modifications, α and β forms.[4] The fiber period 15.60 Å of the α form suggests a fairly large contraction of the molecular chain, while that of the β form 18.9 Å corresponds to the almost fully extended conformation. The α form has a very low crystallite modulus 6 × 10^{10} dyn/cm^2,[5] which is lower by about one order than that of poly(ethylene terephthalate). In the present paper, we determined the molecular and crystal structures of the α form of poly(ethylene oxybenzoate) and discussed the structure–property relationship.

A monoclinic unit cell including a planar zigzag molecular model with the cis CH_2–CH_2 bond,[4] and orthorhombic unit cell with a = 10.46 Å, b = 4.76 Å, c (fiber axis) = 15.60 Å,[5] and the space group $P2_12_12_1$[6] was reported. The crystal structure of the α form, however, has not yet been analyzed successfully, because of difficulty in the setting up of molecular models as will be mentioned in the later sections. Hence we utilized the calculation of the intramolecular interaction energy for selecting suitable molecular models, considering the successful results of application of the energy calculation to the structure analyses: polyisobutylene,[7] poly(*tert*-butylethylene oxide),[8] poly(β-ethyl-β-propiolactone)[9] and so on. In the present study, besides the intramolecular interaction energy calculation, the refinement of the crystal structure model was made by the calculation of intermolecular interaction energy.

Experimental Section

Samples. Uniaxially oriented specimens of the α form for x-ray measurement were prepared by stretching filaments to about 3.5 times the original lengths at 80 °C followed by annealing at 200 °C for 5 h under tension using a metal holder. A doubly oriented specimen was

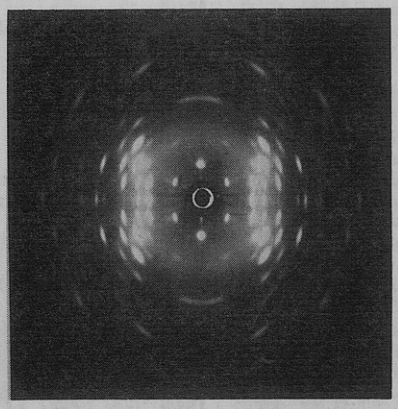

Figure 1. X-ray fiber photograph of poly(ethylene oxybenzoate) α form.

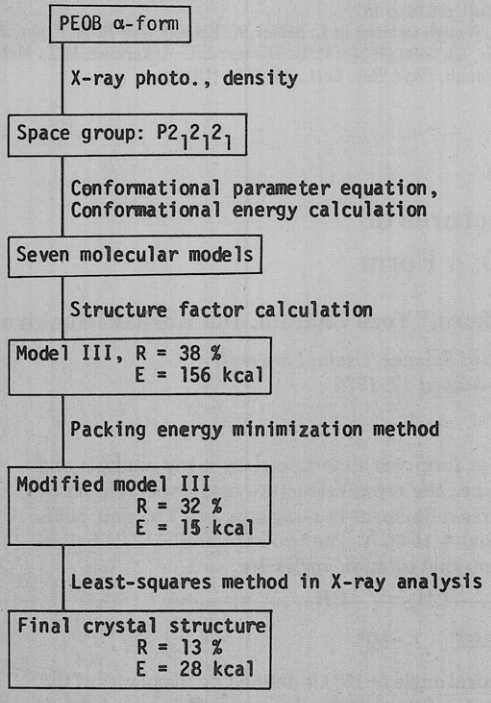

Figure 2. Process of structure determination. R and E are the discrepancy factor and the packing energy, respectively.

obtained by rolling the stretched specimen at room temperature and subsequent annealing between metal plates.

X-Ray Measurements. The nickel-filtered Cu Kα radiation was used throughout the present study. Cylindrical vacuum-cameras of 5 and 10 cm radii were used for measurements of the intensities and spacings, respectively. Figure 1 shows the fiber photograph of the α form. The diffraction intensity measurement was made by the multiple film method, and 145 independent reflections were observed. The reflection intensities were measured by using a microphotometer (Rigaku Denki Co.) and were corrected for the single crystal rotation Lorentz–polarization factor.

Structure Determination. Unit Cell and Space Group. The crystal data were deduced from the fiber photograph and the Weissenberg photograph by using aluminum powder as the calibrating standard for the spacings. The α-form crystal is orthorhombic, and the unit cell dimensions are a = 10.49 Å, b = 4.75 Å, c (fiber axis) = 15.60 Å. From the systematic absences of reflections, $h00$ when h is odd, $0k0$ when k is odd, and $00l$ when l is odd, the space group was found to be $P2_12_12_1$. This space group was confirmed by using the Weissenberg photograph of the doubly oriented specimen. By assuming that four monomeric units are contained in the unit cell, the density is calculated as 1.40 g/cm^3, which is acceptable in comparison with the observed density 1.34 g/cm^3. Thus, it is reasonably assumed that the molecular chain has a twofold screw symmetry relating subsequent monomeric units, and two chains pass through the unit cell.

Table I
Internal Coordinates Assumed for the α Form[a]

	Bond lengths, Å		Bond angles, deg
C(9)–O(2)	1.42	C(9)–O(2)–C(4)	115
O(2)–C(4)	1.37	C(1)–C(7)–O(3)	124
C(1)–C(7)	1.49	O(3)–C(7)–O(1)	122
C(7)–O(3)	1.23	C(1)–C(7)–O(1)	114
C(7)–O(1)	1.36	C(7)–O(1)–C(8)	112
O(1)–C(8)	1.43	O(1)–C(8)–C(9)	109.5
C–C (aliphatic)	1.54	C–C–H (aliphatic)	109.5
C–H	1.09	C–C–C (aromatic)	120
C–C (aromatic)	1.40	C–C–H (aromatic)	120

[a] The atoms are numbered as follows:

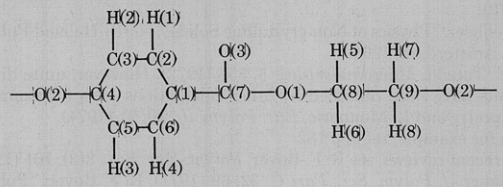

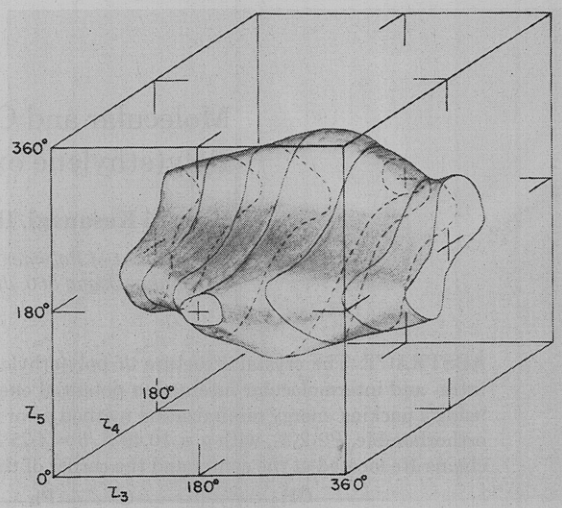

Figure 3. Three-dimensional closed surface for possible conformations of the skeletal chain of the α form in the case of (2/1) helix with the fiber period 15.60 Å.

Process of Structure Determination. The scheme of structure determination is shown in Figure 2. It was rather difficult to set up suitable molecular models of the α form since the contraction of the molecule is fairly large and the number of the internal rotation angles in the skeletal chain is five. As a result, there should be many probable molecular models of quite different conformations. In order to overcome this problem, the molecular conformations, which satisfy the fiber identity period 15.60 Å under the (2/1) helical symmetry, were first examined by using conformational parameter equations which were derived for the present study (see Appendix). Then the intramolecular interaction energy was calculated for these molecular models.

Refinement of the crystal structure model was performed by utilizing the packing energy minimization method[10] followed by the use of the constrained least-squares method of structure factors.[11,12]

Setting Up of Molecular Models. The numbering of the conformational angles is denoted as follows,

$$-O-(-Ph-CO-O-CH_2-CH_2-O-)-$$
$$\tau_1\ \omega\quad \tau_2\ \tau_3\quad \tau_4\quad \tau_5$$

There are five internal rotation angles of the skeletal bonds; τ_1, τ_2, τ_3, τ_4, and τ_5, where τ_1 is for the virtual bond (O–Ph–C), and there is also a dihedral angle ω between the planes of the benzene ring and the ester group. Since the number of the skeletal bonds in the asymmetric unit is five, the independent variables (the internal rotation angles) are

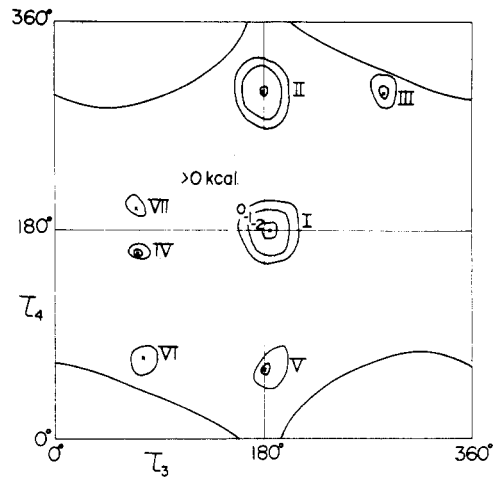

Figure 4. Intramolecular potential energy map plotted against τ_3 and τ_4 of the α form. The upper half of the surface is shown.

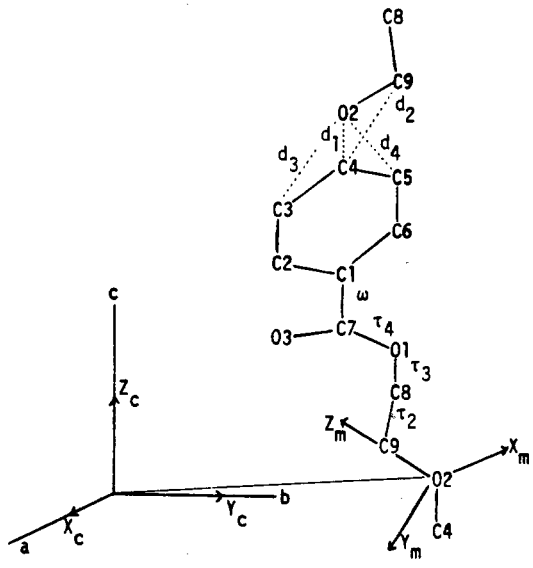

Figure 5. Parameters and constraining conditions used for the refinement by the packing energy minimization method.[10]

three if we use the conformational parameter equations for the (2/1) helix with a fixed fiber period, 15.60 Å. The bond lengths and bond angles used are listed in Table I. If we assume $\tau_2 = 180°$, the possible conformations are limited on the closed surface in the cube defined by the three-dimensional Cartesian coordinates τ_3, τ_4, and τ_5, each covering from 0 to 360° as shown in Figure 3. When τ_3 and τ_4 are given, τ_5 should take two values, under and upper intersecting points on the closed surface, resulting in also a pair of values of τ_1. Furthermore, we considered the dihedral angle ω within the range from −10 to 10°. As the surface has a center of symmetry at $\tau_3 = \tau_4 = \tau_5 = 180°$, the energy calculation can be limited to the upper half of the surface. van der Waals interactions, electrostatic interactions, and internal rotation barriers were taken into account, and the calculation was carried out according to the procedure of the previous work.[13] The potential functions and parameters are the same as those in ref 13 except for the following ones. The van der Waals radius, atomic polarizability, and effective number of outer shell electrons of aromatic carbon atoms were assumed to be 1.8 Å, 1.13×10^{-24} cm^3, and 5.0, respectively. For the internal rotation barriers $[V = V_0(1 - \cos 2\tau)/2]$ of the C(1)–C(7) and C(4)–O(2) bonds, V_0 was taken to be 3.0 and 1.0 kcal/mol, respectively. From the potential energy map shown in Figure 4, seven stable molecular models were obtained as shown in Table II.

Structure Determination. Since two molecular chains pass through the unit cell and the space group $P2_12_12_1$ has four equivalent positions, the chain axis must coincide with a twofold screw axis in the unit cell. Crystal structure models were constructed for the seven models by trial-and-error procedures. The R factors R [$= \Sigma||(I_o)^{1/2}$

Table II
Energetically Stable Molecular Models of the α Form[c]

Model	τ_1, deg	τ_3, deg	τ_4, deg	τ_5, deg	ω, deg	E^a	R^b
I	−82	−175	−180	76	10	−2.1	41
II	65	180	−60	159	0	−2.0	53
III	−41	−75	−60	−164	10	−1.2	38
IV	49	75	160	63	−10	−1.2	48
V	−64	−175	60	107	10	−1.1	48
VI	46	75	70	75	−10	−0.8	59
VII	−59	75	−160	145	10	−0.4	48

[a] Conformational energy, kcal/mol of monomeric unit. [b] Discrepancy factor, %. [c] τ_2 is assumed to be 180°.

Table III
Refinement of the Crystal Structure Model III by the Packing Energy Minimization Method[10]

		Initial	Final
Packing energy, kcal/mol (asym. u.)			
E_a (intramolecular)		9.5	9.5
E_r (intermolecular)		145.9	5.8
E (total)		155.5	15.2
Parameters[a]			
Fractional coordinates of the O(2) atom	x	−0.075	−0.102
	y	0.477	0.570
	z	0.396	0.384
Eulerian angles, deg	θ	113.0	108.7
	ψ	127.5	116.1
	χ	265.9	251.9
Internal rotation angles, deg	τ_4	60.0	76.3
	τ_3	75.0	76.9
	τ_2	180.0	177.3
	ω	−10.0	29.2

[a] Number of independent parameters = (parameters) − (constraining conditions) = 10 − 4 = 6, corresponding to the total number of the two molecular position parameters and the four internal rotation angles. [b] The final internal rotation angles τ_1 = 17.9° and τ_5 = 183.1° were computed from the final coordinates in the minimization process.

Table IV
Atomic Coordinates and Thermal Coefficients of the α Form

Atom	x/a	y/b	z/c	B, Å^2
C(1)	0.1105	0.4470	0.6847	7.2
C(2)	0.0011	0.2851	0.6951	8.7
C(3)	−0.0106	0.1051	0.7666	6.7
C(4)	0.0870	0.0943	0.8277	6.8
C(5)	0.1964	0.2597	0.8173	4.8
C(6)	0.2081	0.4361	0.7458	7.8
C(7)	0.1230	0.6346	0.6087	5.0
C(8)	0.0247	0.8880	0.5006	7.6
C(9)	0.0351	0.7439	0.4125	9.8
O(1)	0.0118	0.6786	0.5659	6.9
O(2)	−0.0752	0.5772	0.3978	12.6
O(3)	0.2239	0.7424	0.5854	11.9
H(1)	−0.0749	0.2899	0.6475	8.0
H(2)	−0.0958	−0.0237	0.7746	8.0
H(3)	0.2724	0.2513	0.8649	8.0
H(4)	0.2932	0.5649	0.7378	8.0
H(5)	−0.0585	0.0256	0.5015	8.0
H(6)	0.1103	0.0120	0.5125	8.0
H(7)	0.0427	0.9037	0.3626	8.0
H(8)	0.1195	0.6101	0.4112	8.0

Table V
Comparison between the Observed and Calculated Intensities[a]

h k l	$(I_o)^{1/2}$	$(I_c)^{1/2}$	*h k l*	$(I_o)^{1/2}$	$(I_c)^{1/2}$	*h k l*	$(I_o)^{1/2}$	$(I_c)^{1/2}$
2 0 0	102	107	1 0 2	5	4	1 4 3		
1 1 0	53	52	2 0 2	38	35	6 3 3	11	13
2 1 0	17	16	0 1 2	50	43	0 4 3		
3 1 0	32	35	1 1 2	168	158	1 0 4	4	8
4 0 0	48	55	2 1 2	81	77	2 0 4	15	10
0 2 0	23	28	3 0 2			0 1 4	24	23
4 1 0	36	40	3 1 2	76	78	1 1 4	46	49
1 2 0			4 0 2	10	12	2 1 4	34	29
2 2 0	-	3	0 2 2	18	22	3 0 4		
3 2 0	-	6	1 2 2	32	28	3 1 4	12	15
5 1 0	-	0	4 1 2			4 0 4	27	36
4 2 0	48	51	2 2 2	14	15	0 2 4	27	24
6 0 0			5 0 2	18	18	1 2 4	37	38
6 1 0	-	10	3 2 2	22	22	4 1 4		
5 2 0	-	13	5 1 2	47	50	2 2 4	35	36
1 3 0	-	7	4 2 2	-	5	5 0 4	25	28
2 3 0	-	4	6 0 2			3 2 4	30	29
7 1 0			6 1 2	-	11	5 1 4	19	10
6 2 0	24	24	5 2 2			4 2 4	31	30
3 3 0			0 3 2	15	19	6 0 4		
4 3 0	-	1	1 3 2			6 1 4	15	18
8 0 0	11	13	2 3 2	21	21	0 3 4		
5 3 0			7 0 2	12	21	1 3 4	9	13
7 2 0	12	10	7 1 2			5 2 4		
8 1 0			6 2 2	14	16	2 3 4	13	16
0 4 0	-	3	3 3 2			7 0 4		
1 4 0	-	8	4 3 2	-	2	3 3 4	-	9
2 4 0			8 0 2	-	3	6 2 4	10	14
6 3 0	14	13	7 2 2			7 1 4		
8 2 0			8 1 2	-	8	4 3 4	11	10
3 4 0			5 3 2			8 0 4	-	0
9 1 0	13	5	0 4 2	-	3	5 3 4		
1 0 1	41	42	6 3 2			7 2 4	18	21
2 0 1	93	96	9 0 2	14	15	8 1 4		
0 1 1	-	14	1 4 2			1 0 5	24	33
1 1 1	69	61	2 4 2			2 0 5	9	21
2 1 1	78	80	3 4 2			0 1 5	-	9
3 0 1			9 1 2	14	14	1 1 5	33	33
3 1 1	10	13	8 2 2			2 1 5	33	33
4 0 1	15	15	1 0 3	16	22	3 0 5		
0 2 1	17	17	2 0 3	25	26	3 1 5	13	9
1 2 1	26	27	0 1 3	-	9	4 0 5	15	21
4 1 1			1 1 3	124	121	0 2 5	58	58
2 2 1	13	15	2 1 3	47	46	1 2 5	42	47
5 0 1	8	11	3 0 3			4 1 5		
3 2 1	25	23	3 1 3	16	14	2 2 5	37	41
5 1 1	25	22	4 0 3	14	17	5 0 5	-	2
4 2 1	26	23	0 2 3	15	11	3 2 5	28	28
6 0 1			1 2 3	26	35	5 1 5	-	10
6 1 1	21	23	4 1 3			6 0 5	15	17
5 2 1			2 2 3	8	10	4 2 5		
1 3 1	20	26	5 0 3	12	19	6 1 5	11	9
0 3 1			3 2 3	14	16	5 2 5		
2 3 1	9	8	5 1 3	19	23	0 3 5	20	22
7 0 1	-	4	4 2 3	25	18	1 3 5		
3 3 1	-	9	6 0 3			2 3 5	-	10
7 1 1			6 1 3	15	18	7 0 5	-	2
6 2 1	13	10	5 2 3	14	22	3 3 5	14	17
4 3 1	-	5	1 3 3			7 1 5		
8 0 1	14	17	0 3 3			6 2 5	-	6
5 3 1			2 3 3	-	14	4 3 5	13	13
7 2 1	11	13	7 0 3	-	14	8 0 5	-	2
8 1 1			3 3 3	17	17	5 3 5		
0 4 1	-	9	7 1 3			7 2 5	13	14
1 4 1			6 2 3	-	5	8 1 5		
2 4 1			4 3 3	-	7	1 0 6	*	25
6 3 1	15	16	8 0 3	-	3	2 0 6	-	1
9 0 1			7 2 3			0 1 6	-	10
8 2 1		6	8 1 3	13	16	1 1 6	61	61
3 4 1	12	14	5 3 3			2 1 6	31	16
9 1 1						0 3 6		

Table V (Continued)

h k l	$(I_o)^{1/2}$	$(I_c)^{1/2}$	h k l	$(I_o)^{1/2}$	$(I_c)^{1/2}$	h k l	$(I_o)^{1/2}$	$(I_c)^{1/2}$
3 1 6	11	10	2 1 7	36	29	4 0 8	-	4
4 0 6	22	28	3 0 7			0 2 8		
0 2 6			3 1 7	27	24	1 2 8	34	25
1 2 6	12	20	4 0 7	-	8	4 1 8		
4 1 6			0 2 7			2 2 8	30	16
2 2 6	24	27	1 2 7	19	17	5 1 8	15	9
3 2 6	26	25	4 1 7			4 2 8	31	26
5 1 6	-	7	2 2 7	20	14	6 0 8		
4 2 6	14	8	5 0 7	-	8	6 1 8	-	2
6 0 6			3 2 7	-	2	5 2 8	-	14
6 1 6	14	13	5 1 7	15	14	0 3 8	-	8
5 2 6			4 2 7	14	13	1 3 8		
0 3 6	15	14	6 0 7			2 3 8	-	7
1 3 6			6 1 7	14	8	7 0 8	-	2
2 3 6			5 2 7			3 3 8	-	4
7 0 6	15	14	0 3 7	14	15	6 2 8	27	13
3 3 6			1 3 7			7 1 8		
7 1 6	-	9	2 3 7	-	9	4 3 8	-	3
4 3 6	14	16	7 0 7	-	0	8 0 8	-	0
6 2 6			3 3 7			5 3 8		
8 0 6	-	6	6 3 7	36	32	7 2 8	24	19
7 2 6			7 1 7			8 1 8		
8 1 6	38	29	1 0 8	*	7	0 0 2	25	23
5 3 6			2 0 8	*	7	0 0 4	18	16
1 0 7	*	20	0 1 8	*	1	0 0 6	29	29
2 0 7	*	6	1 1 8	*	12	0 0 8	11	14
0 1 7	-	5	3 0 8	23	23	0 0 10	17	17
1 1 7	55	57	2 1 8			0 0 12	14	15
			3 1 8	23	19	0 0 14	6	7

[a] The observed structure factors $(I_o)^{1/2}$ were put on the same scale as the $(I_c)^{1/2}$ by setting $\Sigma k(I_o)^{1/2} = \Sigma(mF_c^2)^{1/2}$, where k is the scale factor and m is the multiplicity of the reflections in the fiber photograph. $(I_c)^{1/2}$ of the reflections which overlap on x-ray fiber photograph are $\Sigma(mF_c^2)^{1/2}$. A dash (-) indicates a reflection not observed and an asterisk (*) denotes a reflection whose intensity cannot be observed on fiber photograph.

$-(I_c)^{1/2}|/\Sigma(I_o)^{1/2}]$ for the molecular models are listed in Table II. Among the seven models, model III gave the best agreements between the observed and calculated intensities, but the R factor was still 38%. The poor agreements were considered to suggest the necessity of a fairly large modification of the molecular models obtained by the intramolecular interaction energy calculation alone.

Hereafter, these models were examined by the constrained least-squares method[11,12] in x-ray analysis and the packing energy minimization method.[10] Among them, model III gave the reasonable structure. The process of the structure determination will be described for model III. The refinement of model III by using the constrained least-squares method gave a little better result, R = 26%, but there appeared many unreasonably too close interatomic distances between the neighboring molecular chains, for example, H···H = 1.75 Å, H···C = 1.86 Å, and C···C = 2.90 Å. For overcoming this problem, the packing energy minimization method[10] was applied.

The parameters used for the refinement are shown in Figure 5. Since the bond lengths and bond angles were fixed to the assumed values, there are ten independent variable parameters: three fractional coordinates of the O(2) atom, three Eulerian angles between the coordinate systems $\mathbf{X}_c$ and $\mathbf{X}_m$, and four internal rotation angles τ_2, τ_3, τ_4, and ω. For keeping the bond length and bond angles between successive chain units, we used four constrained distances: d_1 (=1.37 Å), d_2 (=2.43 Å), d_3 (=2.40 Å), and d_4 (=2.40 Å). Model III was used as the initial model of the refinement. After ten minimization cycles, the sum of intra- and intermolecular potential energies, E, was reduced from 156 kcal/mol of asymmetric unit to 15 kcal/mol as shown in Table III. The crystal structure model refined energetically had a good molecular packing, but the R factor was still unsatisfactory, 32%. At the final stage, the constrained least-squares method in x-ray analysis[11,12] was applied for this crystal structure model. The refinable parameters are a scale factor and the 12 isotropic temperature coefficients of the carbon and oxygen atoms, in addition to the 10 structural parameters, are used in the energy minimization refinement. The isotropic temperature coefficients for the hydrogen atoms were fixed to be 8.0 Å.[2] The intensity data of 138 independent reflections were used. The R factor was reduced from 32 to 13%, although the packing energy E becomes a little higher (28 kcal/mol) in the final structure. The final atomic coordinates and the atomic temperature coefficients are listed in Table IV. The observed and calculated structure factors are compared in Table V. The standard deviations are about 0.02 Å for the origin O(2) atom, about 2° for the Eulerian angles, and about 2° for the internal rotation angles.

Results and Discussion

Molecular and Crystal Structures and Crystallite Modulus. The (2/1) helical molecule is shown in Figure 6, in which the internal rotation angles are indicated. The molecular chain was found to take essentially $(CTSGT)_2$ conformation for the skeletal bonds. Accordingly, the chain has a gloss zigzag conformation, one monomeric unit being a large zigzag unit. The internal rotation angle Ph–O was found to be 2° and is much different from that of 50° in poly(phenylene oxide).[14] The crystal structure is shown in Figure 7. There are no abnormally short intermolecular distances. Two antiparallel chains having the benzene rings nearly at the center of the line parts of the zigzag units are located at the corner and the center of the unit cell. The molecular chain having the afore-mentioned conformation is a right- or left-handed helix; two molecular chains passing through the 2_1 positions in a unit cell have the same helix sense. Consequently there may be equal amounts of two kinds of chiral crystallites with the opposite sense.

The molecular conformation should be related with the low observed crystallite modulus of the α form, 6×10^{10} dyn/cm^2 (1 dyn/cm^2 = 10^{-1} Pa),[5] which is lower than the macroscopic modulus 7.2×10^{10} dyn/cm^2.[15] Figure 8 shows the schematic representation of the molecular conformations of poly(ethylene oxybenzoate) α form and poly(ethylene terephthalate),

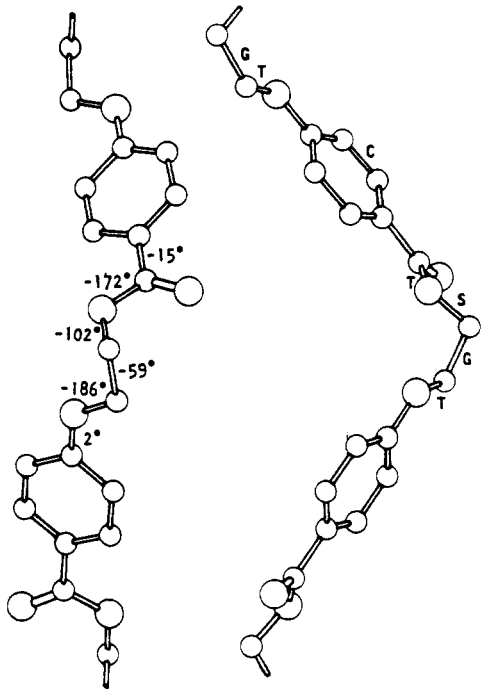

Figure 6. Molecular structure of poly(ethylene oxybenzoate) α form. *C* is the cis conformation for the virtual bond (O–Ph–C).

in which the rigid bonds of molecules are represented by the thick lines. For poly(ethylene oxybenzoate) α form, the deformation of the large zigzag occurs mainly owing to the internal rotation of the three bonds at each turn of the zigzag. Because of the two factors, that is, the long length of the arm, the component of the moment of force, 6 Å, and the smaller values of the internal rotation force constants, the crystallite modulus is small.[16] On the other hand, poly(ethylene terephthalate) has the fairly extended molecular conformation so that the molecular deformation should occur mainly through the changes of the bond angles, and so the modulus is fairly large. The crystallite modulus of poly(ethylene oxybenzoate) α form was calculated to be 2.4×10^{10} dyn/cm^2 for the single chain of the present conformation in this laboratory.[16] Fairly good agreement was obtained between the observed and calculated values, in spite of the calculation for the isolated single chain.

Energy Calculations. The final molecular structure obtained by the analysis was found to be the most similar to model III, which is not the first but third stable molecular model with respect to the intramolecular interaction energy. In Table VI are given the internal rotation angles of the initial model III, the modified model III (obtained by the packing energy minimization method), and the final molecular structure. The values in parentheses are the differences from those of the final structure. If we would not calculate the intramolecular interaction energy, model III would not be found. This initial model III, however, could not converge to the final structure with the subsequent refinement by x-ray analysis, because the differences of the rotation angles from the final structure are fairly large, the average values being 19°. Model III converged eventually to the final structure through the modified model III obtained by the energy minimization method, which reveals the smaller differences (the average values 11°) from the final structure than the initial model III.

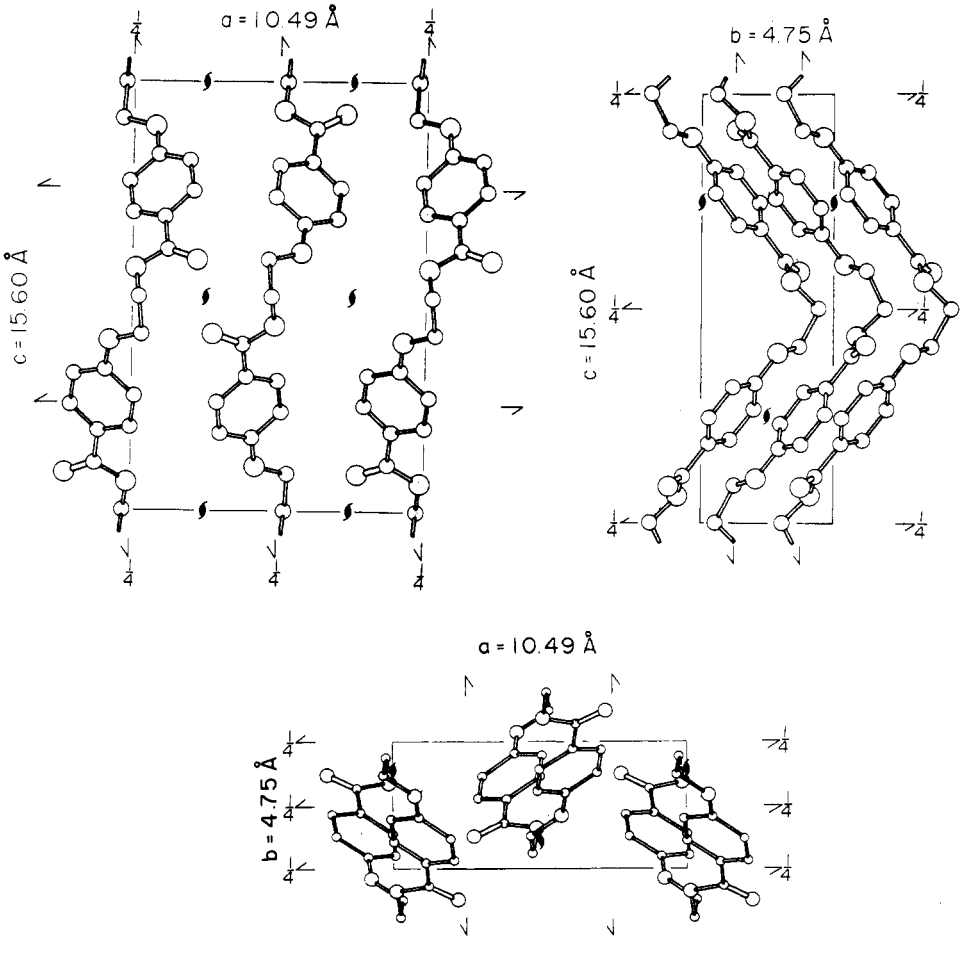

Figure 7. Crystal structure of poly(ethylene oxybenzoate) α form.

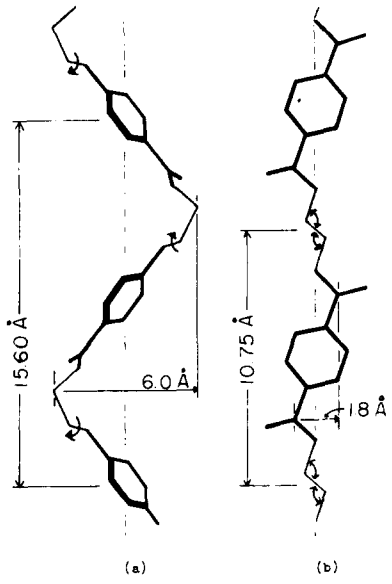

Figure 8. Schematic representation of the molecular structure of (a) poly(ethylene oxybenzoate) α from and (b) poly(ethylene terephthalate).

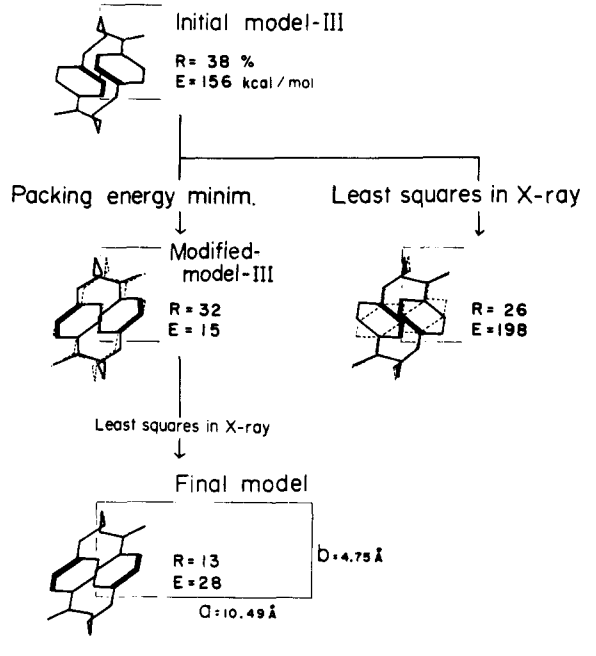

Figure 9. Two ways of refinement of the crystal structure model III. Definitions of R and E are the same as in Figure 2. Broken lines indicate the final molecular structure projected along the c axis.

These relations are also shown in Figure 9, with a schematic representation of a part of the crystal structure models projected along the c axis. The initial model III is as a whole in disagreement with the final structure, especially when the orientation of the benzene rings is evidently incorrect. These facts indicate the significance and the limitation of the intramolecular interaction energy calculation as the method to assume the molecular models for x-ray structure analyses.

In the present study, the packing energy minimization method was used to refine the crystal structure models, i.e., so-called energy refinement.[17] As shown in Figure 9, the orientation of the benzene rings could not be refined successfully

Table VI
Conformational Angles (deg) of Initial Model III, Modified Model III, and Final Molecular Structure

Molecular model	τ_1	τ_2	τ_3	τ_4	τ_5	ω
Model III[a]	−41	−180	−75	−60	−164	10
	(28)[c]	(8)	(27)	(1)	(22)	(25)
Modified model III[b]	−18	−177	−77	−76	−183	−29
	(5)	(5)	(24)	(17)	(3)	(14)
Final structure	−13	−172	−102	−59	−186	−15

[a] Obtained by the intramolecular interaction energy calculation. [b] Obtained by the packing energy minimization method.[10] [c] The values in parentheses indicate the differences from the final structure.

Table VII
The Shifts of the Atoms of the Benzene Ring during the Refinements in Å

Method	C(1)	C(2)	C(3)	C(4)	C(5)	C(6)
Packing energy refinement	0.3	1.2	1.0	0.1	0.8	0.8
Structure factor refinement	0.3	0.4	0.5	0.4	0.4	0.5

after the least-squares refinement in x-ray analysis. On the other hand, the energy refinement rectified the inadequate orientation. This difference may be attributed to the convergence ranges in the two refinement methods. The shifts of the atoms of the benzene ring during the refinements are 0.3–0.5 Å in the refinement in x-ray and 0.1–1.2 Å in the energy refinement, as shown in Table VII. The maximum shift in the latter is almost comparable with the covalent bond distances. The present result indicates that the intermolecular interaction energy calculation plays an important role in the x-ray structure analysis of poly(ethylene oxybenzoate) α form.

Appendix

Derivation of Conformational Parameter Equations for (2/1) Helix. When the number of skeletal chain atoms in the chemical unit is k for a (2/1) helical chain with a fixed identity period, the number of independent internal rotation angles is $(k - 2)$, although the methods[18-21] for calculating the molecular conformations so far needed k or $(k - 1)$ rotation angles. When these methods are used, the helical parameters, i.e., the translation of one chemical unit along the helix axis d and/or the rotation angle about the axis per chemical unit θ (=180°), should be calculated approximately by trial and graphically. The present method can give the conformations directly under the fixed values of d and θ.

The numbering of the conformational parameters is shown in Figure 10, where r_j, ϕ_j, and τ_j denote the jth bond length, bond angle, and internal rotation angle, respectively. A right-handed coordinate system $\mathbf{X}$ is defined as the basic coordinate system so that the first atom is fixed at the origin, the second atom lies on the X axis, and the third atom is on the XY plane. Here $\mathbf{X}(j)$ is the coordinates of the jth atom in the $\mathbf{X}$ coordinate system. The relationship between $\mathbf{X}(j-1)$ and $\mathbf{X}(j)$ can be represented by the following recursion formula

$$\mathbf{X}(j) = \mathbf{A}_2{}^{\phi}\mathbf{A}_2{}^{\tau} \ldots \mathbf{A}_{j-2}{}^{\tau}\mathbf{A}_{j-1}{}^{\phi}\mathbf{B}_j + \mathbf{X}(j-1) \quad (j \geq 4) \tag{1}$$

where

$$\mathbf{X}(1) = \begin{bmatrix} 0 \\ 0 \\ 0 \end{bmatrix}, \mathbf{X}(2) = \begin{bmatrix} r_1 \\ 0 \\ 0 \end{bmatrix}, \mathbf{X}(3) = \begin{bmatrix} -r_2 \cos \phi_2 + r_1 \\ r_2 \sin \phi_2 \\ 0 \end{bmatrix},$$

$$\mathbf{A}_j{}^{\phi} = \begin{bmatrix} -\sin \phi_j & -\sin \phi_j & 0 \\ \sin \phi_j & -\cos \phi_j & 0 \\ 0 & 0 & 1 \end{bmatrix},$$

$$\mathbf{A}_j{}^{\tau} = \begin{bmatrix} 1 & 0 & 0 \\ 0 & \cos \tau_j & -\sin \tau_j \\ 0 & \sin \tau_j & \cos \tau_j \end{bmatrix}, \mathbf{B}_j = \begin{bmatrix} r_j \\ 0 \\ 0 \end{bmatrix}$$

We assume k bond lengths, k bond angles, $(k-2)$ internal rotation angles, i.e., $\tau_2, \tau_3, \cdots, \tau_{k-1}$, and the value of a fiber identity period, c, as already determined, and the remaining two internal rotation angles, τ_k, τ_{k+1} $(=\tau_1)$, as undetermined. The coordinates of the $(k+1)$th atom in the **X** coordinate system can be expressed by using the values of $\tau_2, \tau_3, \cdots, \tau_{k-1}$.

$$\mathbf{X}(k+1) = \mathbf{A}_2{}^{\phi}\mathbf{A}_2{}^{\tau} \ldots \mathbf{A}_{k-1}{}^{\tau}\mathbf{A}_k{}^{\phi}\mathbf{B}_k + \mathbf{X}(k) = \begin{bmatrix} X(k+1) \\ Y(k+1) \\ Z(k+1) \end{bmatrix} \tag{2}$$

The direction cosine vector $\mathbf{L}_{k+1}$ of the bond r_{k+1} in the **X** coordinate system is given by eq 3, which contains the undetermined parameter τ_k.

$$\mathbf{L}_{k+1} = \begin{bmatrix} l_{k+1} \\ m_{k+1} \\ n_{k+1} \end{bmatrix} = [\mathbf{X}(k+2) - \mathbf{X}(k+1)]/\mathbf{B}_{k+1}$$

$$= \mathbf{A}_2{}^{\phi}A_2{}^{\tau} \ldots \mathbf{A}_k{}^{\tau}\mathbf{A}_{k+1}{}^{\phi} \begin{bmatrix} 1 \\ 0 \\ 0 \end{bmatrix}$$

$$= \begin{bmatrix} a_{11} + a_{12} \cos \tau_k + a_{13} \sin \tau_k \\ a_{21} + a_{22} \cos \tau_k + a_{23} \sin \tau_k \\ a_{31} + a_{32} \cos \tau_k + a_{33} \sin \tau_k \end{bmatrix} \tag{3}$$

If the direction cosines of the helix axis $\mathbf{L}_a$ are assumed as follows in the **X** coordinate system,

$$\mathbf{L}_a = \begin{bmatrix} l_a \\ m_a \\ n_a \end{bmatrix}$$

the translation of the one chemical unit along the axis, d $(=c/2)$, is represented by eq 4.

$$d = |\mathbf{L}_a\, \mathbf{X}(k+1)| = l_a X(k+1) + m_a Y(k+1) + n_a Z(k+1) \tag{4}$$

Under the condition of (2/1) helical symmetry, the three unit vectors $\mathbf{L}_1$, $\mathbf{L}_{k+1}$, and $\mathbf{L}_a$ are on a same plane, and the vector $\mathbf{L}_a$ bisects the angle between the vectors $\mathbf{L}_1$ and $\mathbf{L}_{k+1}$. Therefore, from the relation $\mathbf{L}_1 \times \mathbf{L}_a = \mathbf{L}_a \times \mathbf{L}_{k+1}$ that is

$$\begin{bmatrix} 1 \\ 0 \\ 0 \end{bmatrix} \times \begin{bmatrix} l_a \\ m_a \\ n_a \end{bmatrix} = \begin{bmatrix} l_a \\ m_a \\ n_a \end{bmatrix} \times \begin{bmatrix} l_{k+1} \\ m_{k+1} \\ n_{k+1} \end{bmatrix}$$

the following equations are derived.[22]

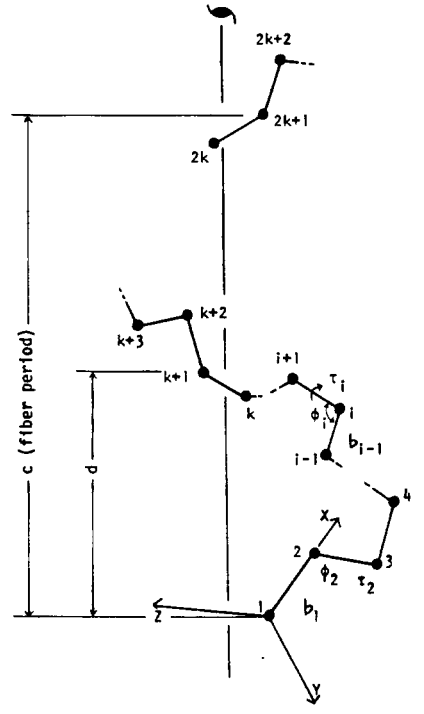

Figure 10. A (2/1) helical chain in the **X** coordinate system and the numbering of conformational parameters.

$$l_a = [(l_{k+1} + 1)/2]^{1/2}$$

$$m_a = m_{k+1}/[2(l_{k+1} + 1)]^{1/2}$$

and

$$n_a = n_{k+1}/[2(l_{k+1} + 1)]^{1/2} \tag{5}$$

By substituting eq 5 to eq 4, we have

$$[2(l_{k+1} + 1)]^{1/2}d = (l_{k+1} + 1)X(k+1) + m_{k+1}Y(k+1) + n_{k+1}Z(k+1) \tag{6}$$

Equation 6 can be expressed by using eq 3 in terms of $a_{11}, a_{12}, a_{13}, \ldots, a_{33}$, and τ_k, and the following trigonometrical equation is obtained.

$$[2(1 + a_{11} + a_{12} \cos \tau_k + a_{13} \sin \tau_k)]^{1/2}d = [1 + a_{11} + a_{12} \cos \tau_k + a_{13} \sin \tau_k]\, X(k+1) + [a_{21} + a_{22} \cos \tau_k + a_{23} \sin \tau_k]Y(k+1) + [a_{31} + a_{32} \cos \tau_k + a_{33} \sin \tau_k]Z(k+1) \tag{7}$$

By solving this trigonometrical equation, two values of τ_k are obtained numerically.

Next we must calculate the following matrices.

$$\mathbf{A}_1{}^{\tau}\mathbf{A}_1{}^{\phi}\mathbf{A}_2{}^{\tau}\mathbf{A}_2{}^{\phi} \ldots \mathbf{A}_k{}^{\tau}\mathbf{A}_k{}^{\phi} = \begin{bmatrix} 1 & 0 & 0 \\ 0 & \cos \tau_1 & -\sin \tau_1 \\ 0 & \sin \tau_1 & \cos \tau_1 \end{bmatrix} \times \begin{bmatrix} c_{11} & c_{12} & c_{13} \\ c_{21} & c_{22} & c_{23} \\ c_{31} & c_{32} & c_{33} \end{bmatrix} \tag{8}$$

in which the trace of the matrices is equal to -1 for (2/1) helical symmetry. Hence we obtain eq 9.

$$1 + c_{11} + (c_{22} + c_{33}) \cos \tau_1 + (c_{23} - c_{32}) \sin \tau_1 = -1 \tag{9}$$

The remaining conformational parameter τ_1 is determined

by solving this quadratic equation, using the values of τ_k. Consequently two sets of solutions are obtained for the parameters τ_1 and τ_k, if

$$[X(k+1)^2 + Y(k+1)^2 + Z(k+1)^2]^{1/2} \leqq d$$

This procedure could save a lot of computation for setting up molecular models of (2/1) helical chains such as poly(ethylene oxybenzoate) α form.

References and Notes

(1) Faculty of Science and Engineering, Saga University, Saga, Japan.
(2) R. de P. Daubeny and C. W. Bunn, *Proc. R. Soc. London, Ser. A*, **226**, 531 (1954).
(3) I. Sakurada and K. Kaji, *Kobunshi Kagaku*, **26**, 817 (1969).
(4) M. Korematsu and S. Kuriyama, *Nippon Kagaku Zasshi*, **81**, 917 (1969).
(5) I. Sakurada, K. Nakamae, K. Kaji, and S. Wadano, *Kobunshi Kagaku*, **26**, 561 (1969).
(6) F. Ikejiri, K. Iohara, S. Takamuku, K. Suehiro, K. Imada, and M. Takayanagi, 17th Annual Meeting of the Polymer Society of Japan, Tokyo, Japan, 1968, Abstract p 456.
(7) G. Allegra, E. Benedetti, and C. Pedone, *Macromolecules*, **3**, 727 (1970).
(8) H. Sakakihara-Kitahama and H. Tadokoro, *J. Macromol. Sci., Phys.*, **9**, 511 (1974).
(9) M. Yokouchi, Y. Chatani, H. Tadokoro, and H. Tani, *Polym. J.*, **6**, 248 (1974).
(10) H. Kusanagi, H. Tadokoro, and Y. Chatani, *Rep. Prog. Polym. Phys. Jpn.*, **18**, 193 (1975).
(11) S. Arnott and A. J. Wonacott, *Polymer*, **7**, 157 (1966).
(12) Y. Takahashi, T. Sato, H. Tadokoro, and Y. Tanaka, *J. Polym. Sci., Polym. Phys. Ed.*, **11**, 233 (1973).
(13) H. Tadokoro, K. Tai, M. Yokoyama, and M. Kobayashi, *J. Polym. Sci., Polym. Phys. Ed.*, **11**, 825 (1973).
(14) J. Boon and E. D. Magré, *Makromol. Chem.*, **126**, 130 (1969).
(15) M. Ichihara, private communication.
(16) K. Tashiro, M. Kobayashi, and H. Tadokoro *Macromolecules*, in press.
(17) M. Levitt, *J. Mol. Biol.*, **82**, 393 (1974).
(18) T. Shimanouchi and S. Mizushima, *J. Chem. Phys.*, **23**, 707 (1955).
(19) T. Miyazawa, *J. Polym. Sci.*, **39**, 746 (1961).
(20) H. Sugeta and T. Miyazawa, *Biopolymers*, **5**, 673 (1967).
(21) M. Yokouchi, H. Tadokoro, and Y. Chatani, *Macromolecules*, **7**, 769 (1974).
(22) In the case of $l_{k+1} = -1$, eq 5 becomes undetermined. However, the value of τ_k is directly calculated from eq 3.

Elastic Moduli and Molecular Structures of Several Crystalline Polymers, Including Aromatic Polyamides

Kohji Tashiro, Masamichi Kobayashi, and Hiroyuki Tadokoro*

Department of Polymer Science, Faculty of Science, Osaka University, Toyonaka, Osaka 560, Japan.

Received September 2, 1976

ABSTRACT: The relationship between the elastic moduli and the molecular structures has been investigated for three typical aromatic polyamides, poly(*p*-phenyleneterephthalamide), poly-*p*-benzamide, and poly(*m*-phenyleneisophthalamide), and related polymers, poly(ethylene terephthalate), etc. Potential energy calculations of the aromatic polyamides indicate very high potential barrier hindering conformational changes and suggest the presence of extended molecules in noncrystalline regions for poly(*p*-phenyleneterephthalamide) and poly-*p*-benzamide, causing the very high values of the measured macroscopic moduli. The calculated crystallite moduli agree well with the observed values. The distributions of the strain potential energy to the internal coordinates, that is, the changes of the bond lengths, bond angles, and internal rotation angles, have been calculated. The relation between the crystallite moduli and macroscopic moduli for various polymers is discussed in connection with the molecular conformations in the crystalline region and the orderness and mobility of the molecules in the amorphous region.

Fibers made of poly(*p*-phenyleneterephthalamide) (commercial name of du Pont Kevlar or Fiber B) and poly-*p*-benzamide (PRD-49 Type I, abbreviated as PRD-49 hereafter) have characteristic properties such as high tensile strength, high elastic modulus, and high thermal resistance, as shown in Table I. Poly(*m*-phenyleneisophthalamide) fiber (Nomex) is excellent in heat stability, although it shows an elastic modulus and tensile strength similar to usual fibers.[1,2] These characteristic features can be reasonably interpreted by the results of structure analyses.

In this paper we focus our attention mainly into the elastic moduli of these aromatic polyamides and related polymers including poly(ethylene terephthalate) and poly(ethylene oxybenzoate), which have the benzene rings in the skeletal chains. The crystallite modulus was first measured by Dulmage and Contois[9] on poly(ethylene terephthalate) based upon the assumption of series model. Thereafter the study was extended for a wide variety of polymers by Sakurada and his co-workers.[4] In Table I are shown the measured crystallite moduli (CM) of several polymers including Kevlar and Nomex by Sakurada et al.[5] The crystallite modulus can be calculated theoretically if the geometrical structure is known and the suitable force constants can be assumed. This calculation was first made by Mark[10] for straight-chain hydrocarbon and also by Meyer[11] for cellulose. Then, Treloar,[12] Shimanouchi,[13] Miyazawa[14] and the others made the calculations for many polymers. We calculated the crystallite moduli of the single molecular chains of the aromatic polyamides and related polymers based on the crystal structures determined by x-ray analyses and examined the relationships among the elastic moduli, the molecular conformations, and the flexibility of the chains.

Chain Conformations and Flexibility

The crystal structures of Kevlar,[1] PRD-49,[1] and Nomex[2] are reproduced in Figures 1, 2, and 3, respectively, and their crystallographic data are given in Table II.

The molecular conformation of Kevlar in the crystalline region is fully extended all trans.

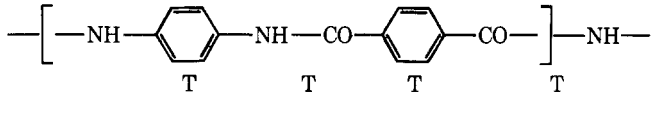

Here we replace N–Ph–N or C–Ph–C by a virtual bond after Flory.[15] The internal rotational angles (ω) of the benzene ring measured from the amide plane are about 30°.